

[Note: This is a draft of a manuscript. Contents of this document should not be quoted or referred to without permission of the author(s).]

Invited paper presented at the 130th Annual Meeting & Exhibition of the Minerals, Metals, and Materials Society (TMS) in New Orleans, Louisiana, February 11-15, 2001.

The Role of Ledge Nucleation/Migration in Ω Plate Thickening Behavior in Al-Cu-Mg-Ag Alloys

C. R. Hutchinson¹, X. Fan^{2,3}, S. J. Pennycook³, and G. J. Shiflet¹

¹Department of Materials Science and Engineering
University of Virginia
Charlottesville, Virginia 22903

²Department of Chemical and Material Engineering
University of Kentucky
Lexington, Kentucky 40506

³Solid State Division
Oak Ridge National Laboratory
P.O. Box 2008
Oak Ridge, Tennessee 37831-6030

"The submitted manuscript has been authored by a contractor of the U.S. Government under contract No. DE-AC05-00OR22725. Accordingly, the U.S. Government retains a nonexclusive, royalty-free license to publish or reproduce the published form of this contribution, or allow others to do so, for U.S. Government purposes."

Prepared by the

SOLID STATE DIVISION
OAK RIDGE NATIONAL LABORATORY
Managed by
UT-BATTELLE, LLC, for the
U.S. DEPARTMENT OF ENERGY
Under Contract DE-AC05-00OR22725

March 2001

THE ROLE OF LEDGE NUCLEATION/MIGRATION IN Ω PLATE THICKENING BEHAVIOUR IN Al-Cu-Mg-Ag ALLOYS

¹C. R. Hutchinson, ^{2,3}X. Fan, ³S. J. Pennycook and ¹G. J. Shiflet

¹Dept. of Mat. Sci. and Eng., University of Virginia, Charlottesville, VA, 22903, USA.

²Dept. of Chem. and Mat. Eng., University of Kentucky, Lexington, KY, 40506, USA.

³Solid State Division, Oak Ridge National Laboratory, Oak Ridge, TN, 37831, USA.

Abstract

The thickening kinetics of Ω plates in an Al-4Cu-0.3Mg-0.2Ag (wt. %) alloy have been measured at 200 °C, 250 °C and 300 °C using conventional transmission electron microscopy techniques. At all temperatures examined the thickening showed a linear dependence on time. At 200 °C the plates remained less than 6nm in thickness after 1000h exposure. At temperatures above 200 °C the thickening kinetics are greatly increased. Atomic resolution Z-contrast microscopy has been used to examine the structure and chemistry of the $(001)_{\Omega} \parallel (111)_{\alpha}$ interphase boundary in samples treated at each temperature. In all cases, two atomic layers of Ag and Mg segregation were found at the broad face of the plate. The risers of the growth ledges and the ends of the plates were free of segregation. No significant levels of Ag or Mg were detected inside the plate at any time. The necessary redistribution of Ag and Mg accompanying a migrating thickening ledge occurs at all temperatures and is not considered to play a decisive role in the excellent coarsening resistance exhibited by the Ω plates at temperatures up to 200 °C. Plates transformed at 200 °C rarely contained ledges and usually exhibited a strong vacancy misfit normal to the plate. A large increase in ledge density was observed on plates transformed at 300 °C, concomitant with accelerated plate thickening kinetics. The high resistance to plate coarsening exhibited by Ω plates at temperatures up to 200 °C, is due to limited ledge nucleation under these conditions. The prohibitively high barrier to coherent ledge nucleation on the broad faces of plates aged at 200 °C arises from the contribution to the total free energy change attending nucleation from elastic interactions between the misfitting coherent ledges and the significant strain field that can exist normal to the broad face of the Ω plate.

Acknowledgments

CRH and GJS greatly acknowledge the support of the Southeastern Universities Research Association 1999 Summer Cooperative Research Program and the National Science Foundation under grant number DMR-9904034. The work at Oak Ridge National Laboratory was supported by the Division of Materials Sciences, US Department of Energy under contract No. DE-AC05-00OR22725 with UT-Battelle, LLC. Dr. Simon Ringer of the Electron Microscopy Unit at the University of Sydney, Australia is thanked for kind provision of materials used in this study.

1. Introduction

The addition of trace amounts of Ag to Al-Cu-Mg alloys with high Cu:Mg ratios (eg., 10:1) significantly alters the precipitation sequence usually observed in these alloys [1-4]. The most notable change is the appearance of a thin, hexagonal-shaped phase, designated Ω , that forms as platelets on the $\{111\}_\alpha$ slip planes of the matrix. Several structures for the Ω phase have been proposed [5-7] although the most widely accepted structure is orthorhombic (Fmmm, $a=0.496\text{nm}$, $b=0.859\text{nm}$, $c=0.848\text{nm}$) [8, 9]. The orientation relationship between Ω and the α matrix is $(111)_\alpha \parallel (001)_\Omega$ and $[\bar{1}10]_\alpha \parallel [010]_\Omega$. The appearance of the Ω phase promotes greater hardening, and alloys based on the Al-Cu-Mg-Ag system have shown promising creep properties at temperatures up to 200 °C because of the apparent resistance of the Ω phase to particle coarsening [10]. The reported coarsening resistance of Ω has been confirmed by Ringer *et al.* [11]. Those researchers directly measured the changes in plate thickness using conventional transmission electron microscopy (CTEM) techniques as a function of time for temperatures between 200 °C and 300 °C. The plates examined in that study remained less than 6nm in thickness after 1000h exposure at 200 °C. At temperatures above 200 °C the thickening was greatly accelerated.

It is now generally accepted that rationally oriented plate-like precipitates thicken by a ledge mechanism [12] (Fig. 1). The thickening of plate-like precipitates therefore depends on the kinetics of the *nucleation and growth of thickening ledges* on the broad faces of the plates. Previous studies on precipitate thickening kinetics in Al-alloys [13-15] have concluded that the overall thickening kinetics are ultimately restricted by limited ledge nucleation.

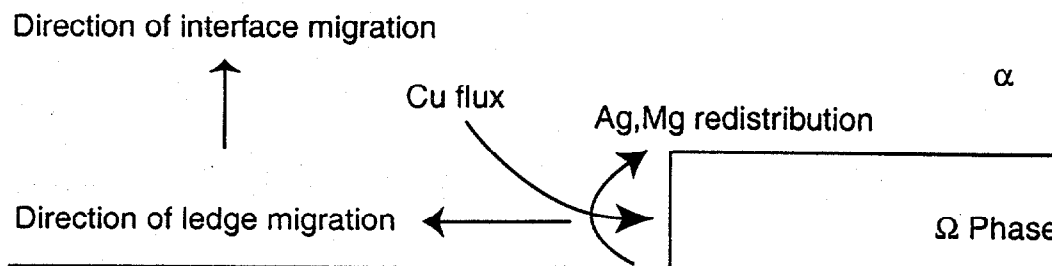


Figure 1. Schematic illustration of the necessary Ag and Mg redistribution and Cu flux accompanying the migration of a thickening ledge on an Ω plate.

Ω plates differ from other $\{111\}_\alpha$ precipitate plates in at least two important aspects. The first concerns the relatively large lattice misfit between the precipitate and the matrix that exists normal to the $(111)_\alpha \parallel (001)_\Omega$ interphase boundary. Other examples of $\{111\}_\alpha$ plates include T_1 (Al_2CuLi) in Al-Cu-Li alloys, η' (MgZn_2) in Al-Zn-Mg and γ' (γ) (AlAg_2) in Al-Ag. Each of these phases has a hexagonal structure whereas Ω is usually assumed to be hexagonal. The misfit normal to the precipitate for each of these phases is 0.12% for T_1 , 0.03% for η' , 1.46% for γ' and 9.3% for Ω . The misfit normal to the Ω plate is accordingly considered large. On the basis of this large misfit, Fonda *et al.* [16] initially postulated that the source of the enhanced thermal stability of Ω may be the relationship between ledge nucleation and propagation and the elastic strain field. Fonda *et al.* [16] investigated the accommodation of misfit strain surrounding Ω plates and found the plates consistently exhibit a vacancy type strain field normal to the habit plane (Fig. 2), independent of plate thickness. Two types of thickening ledges were observed, coherent $1/2\Omega$ unit cell high ledges and less commonly, larger ledges which contain a misfit compensating dislocation of the type $b=1/3\langle 111 \rangle_\alpha$. Similar dislocations were also

observed at the ends of the plates with an average spacing of $2\frac{1}{2}$ or 3Ω unit cells, which produces a minimum strain normal to the plate.

The second characteristic that differentiates Ω from other $\{111\}_\alpha$ plates is the well reported segregation of Ag and Mg to the broad face of the Ω plate. This segregation was first detected by Muddle and Polmear [9] and most recently by Reich *et. al.* [17] using 3D-APFIM. The 3D-APFIM work of Reich *et. al.* has provided evidence to warrant careful consideration of the usual assumption that ledge nucleation controls the overall plate thickening rate in Al-based alloys. In Reich *et. al.*'s atom probe study, they captured an Ω plate thickening ledge in an Al-1.9Cu-0.3Mg-0.2Ag (at. %) alloy aged 10h at 180 °C. Their observations show the presence of a monoatomic layer of Ag and Mg at the Ω plate/matrix $(001)_\Omega \parallel (111)_\alpha$ interface but no Ag or Mg was detected within the plate itself or at the riser of the ledge. The motion of the thickening ledge must then involve the simultaneous flux of Cu from the matrix to the riser of the ledge and the redistribution of Ag and Mg from the original broad face of the Ω plate to the terrace of the migrating thickening ledge. Fig. 1 is a schematic illustration of this process¹. This complicated diffusion geometry raises two interesting questions. (a) What interaction (if any) is there between the redistributing Ag and Mg and the incoming flux of Cu? and (b) If an interaction is expected, could it be sufficient to retard ledge migration to the point where it becomes the rate controlling process for plate thickening instead of ledge nucleation?

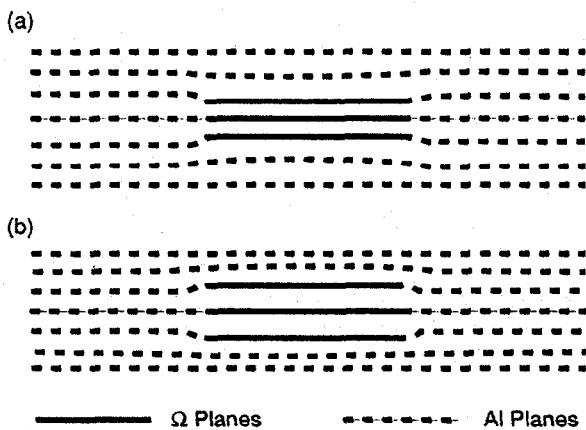


Figure 2. Schematic illustration of (a) vacancy and (b) interstitial strain fields normal to the broad face of a precipitate plate.

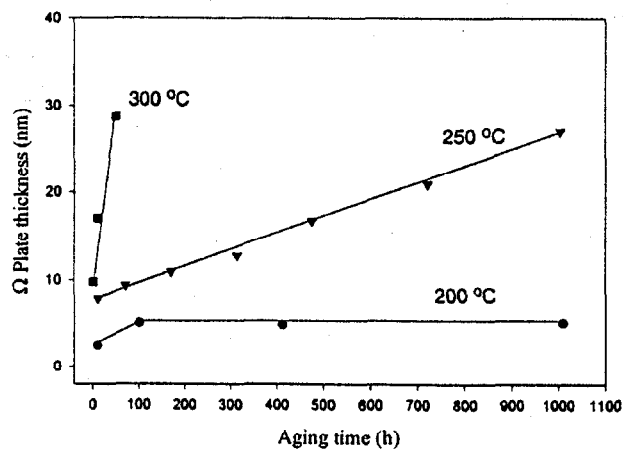


Figure 3. Mean Ω plate thickness (nm) as a function of time at 200 °C, 250 °C and 300 °C, in an Al-4Cu-0.3Mg-0.4Ag (wt. %) alloy.

The present work addresses the need for a systematic study of the structure and chemistry of the Ω plate/matrix $(001)_\Omega \parallel (111)_\alpha$ interface as a function of time and temperature to examine the respective roles of ledge nucleation and migration in accounting for the excellent coarsening resistance of Ω plates at temperatures up to 200 °C.

1. The diffusion path for Ag and Mg redistribution from the broad face of the plate to the terrace of the migrating thickening ledge shown in Fig. 1 is only one of several possible diffusion paths. This schematic is not intended to imply that this is the path of solute redistribution, only that some interaction between the flux of Cu and the Ag and Mg may be expected.

2. Experimental Procedure

The composition of the alloy used is Al-4.0Cu-0.3Mg-0.4Ag (wt. %). Strips of material 0.5-1mm thick were solution treated (ST) at 525 °C for 1h, water quenched (WQ) and aged in molten salt baths at 200 °C ± 2°C, 250 °C ± 2°C or 300 °C ± 2°C for various times up to 1000h.

Specimens for transmission electron microscopy (TEM) were punched mechanically from the strips and twin-jet electrolytically polished in a solution of 33 vol. % nitric acid and 67 vol. % methanol at -25 °C. The microstructural evolution was monitored using CTEM techniques with a 200 kV microscope. High resolution phase contrast microscopy was performed using a top entry HREM operating at 400 kV. The high resolution phase contrast simulation was performed using the Crystalkit and MacTempas software packages [18]. Atomic resolution Z-contrast microscopy [19, 20] was used for the systematic examination of the composition and structure of the Ω plate/matrix $(001)_{\Omega} \parallel (111)_{\alpha}$ interface as a function of time and temperature. This technique is capable of providing two-dimensional intuitively interpretable images of atomic structures with compositional sensitivity without the need for model structures and simulations associated with the phase contrast imaging techniques. A Z-contrast image is formed by scanning an electron probe of atomic dimensions across a specimen and collecting the high angle scattered electrons with an annular dark-field (HAADF) detector. Since the scattering is incoherent at high scattering angles, the image is essentially a map of the total scattering intensity of each atomic column, which is approximately proportional to the square of the atomic number (Z). This technique is especially well suited to the investigation of Ag in the Al-Cu-Mg-Ag system due to the relatively high atomic number of Ag. The microscopy was performed using a VG Microscope HB603U scanning transmission electron microscope operating at 300kV which is capable of forming an electron probe size of 0.126nm. The EDS analysis was carried out using a ATEM operating at 200 kV equipped with a field emission gun and an EDSX system.

Measurements of the thickness of Ω precipitate plates were made from CTEM micrographs recorded with the electron beam parallel to the precipitate habit plane (i.e. parallel to $\langle 112 \rangle_{\alpha} // [100]_{\Omega}$ or $[110]_{\Omega}$). In each case, the "edge-on" thickness of between 70 and 100 precipitates was measured from the negatives magnified using a 4x graticule.

3. Results

3.1 Conventional Transmission Electron Microscopy (CTEM)

Observations of the $\langle 100 \rangle_{\alpha}$, $\langle 110 \rangle_{\alpha}$ and $\langle 112 \rangle_{\alpha}$ zone axes of the Al matrix were made to ensure a true representation of the precipitate distribution was obtained. At all times and temperatures examined, the Ω phase was found to be present. At 200 °C and 250 °C, the Ω phase coexists with θ' (Al_2Cu) and S (Al_2CuMg) phases. At 300 °C, the Ω phase was the only precipitate found at all times observed. The thickening kinetics of Ω plates were measured at each temperature. A plot of plate thickness as a function of time is shown in Fig. 3. At all temperatures examined the precipitate thickness shows a linear dependence on time. At 200 °C, the Ω plates reach a thickness of approximately 5.5nm after 100h exposure, after which there is no detectable change in average thickness. At 300 °C the rate of thickening is rapid and thicknesses greater than 30nm are reached within 50h at 300 °C. At 250 °C, thicknesses of 25-30nm are obtained after 1000h exposure. These observations are qualitatively consistent with those of Ringer *et al.* [11].

3.2 High Resolution Electron Microscopy

3.2.1 Z-Contrast Microscopy

Atomic resolution Z-contrast microscopy was used to examine the structure and chemistry of the Ω plate/matrix $(001)_{\Omega} \parallel (111)_{\alpha}$ interface in samples transformed at each temperature.

A low magnification Z-contrast image of an Ω plate (right) and a θ' plate (left) is presented in Fig. 4(a). The intensity in a Z-contrast image is approximately proportional to Z^2 and the bright bands bounding each side of the Ω plate are interpreted as preferential segregation of at least Ag to the Ω plate/matrix $(001)_{\Omega} \parallel (111)_{\alpha}$ interphase boundary, consistent with previous investigations [9, 17]. Ω plates in this orientation (Fig. 4(a)) were found to be very long, straight and typical of Ω plates observed in samples transformed at 200 °C. An atomic resolution Z-contrast image of a 4 unit cell thick Ω plate is shown in Fig. 4(b). Two atomic layers of enhanced intensity are seen at the Ω plate/matrix $(001)_{\Omega} \parallel (111)_{\alpha}$ interface. These correspond to two layers of segregation. This is in contrast to the monoatomic layer reported by Reich *et al.* [17]. The layers of enhanced intensity within the plate parallel to the habit plane are separated by 0.424 nm and correspond to layers enriched in Cu. This is qualitatively consistent with the projection of the proposed orthorhombic Ω structure down zone axes parallel to the habit plane. EDS was used to determine that the interfacial segregation contained both Ag and Mg, consistent with recent analytical investigations [17]. No significant quantities of Ag or Mg were detected within the Ω plate or the adjacent matrix.

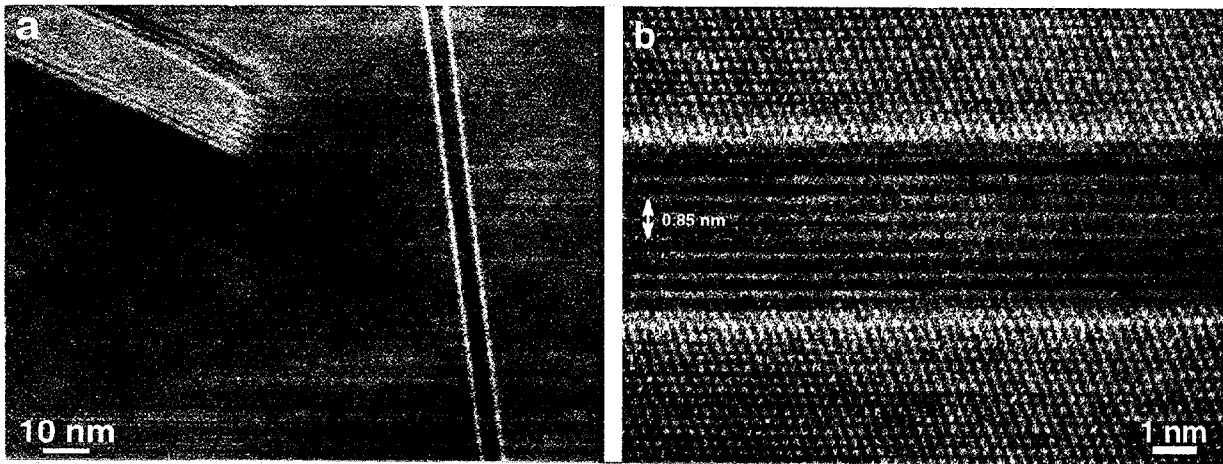


Figure 4. Z-contrast images of sample transformed 100h at 200 °C. (a) Low magnification image of Ω plate (right) and θ' plate (left). (b) Atomic resolution image of an Ω plate illustrating two atomic layers of interfacial segregation.

Fig. 5(a) is a Z-contrast image of an Ω plate thickening ledge in a sample exposed for 70h at 250 °C. The ledge is $1/2$ Ω unit cell high and coherent with the matrix. The image shows a double layer of interfacial segregation to the terraces of the growth ledge but not at the riser of the ledge. The lack of segregation at the riser of the thickening ledge is consistent with the APFIM observations of Reich *et al.* [17]. Energy dispersive spectra were obtained from the matrix, the $(001)_{\Omega} \parallel (111)_{\alpha}$ interphase boundary and wholly within the Ω plate. They showed segregation of both Ag and Mg to the interface. As was the case for the sample treated at 200 °C, no significant quantities of Ag or Mg were detected within the Ω plate or the adjacent matrix. At 300 °C the Ω plates thickened at a greatly enhanced rate, and the Z-contrast image in Fig. 5(b) shows thickening ledges are plentiful on Ω plates transformed at this temperature. Two atomic layers of segregation to the Ω plate/matrix $(001)_{\Omega} \parallel (111)_{\alpha}$ interface were again observed. EDS analysis

confirmed that the intensity seen at the plate/matrix interface in the Z-contrast image was due to both Ag and Mg segregation. No significant quantities of Ag or Mg were detected within the plate or adjacent matrix. Different sized ledges can be observed on the broad faces of the Ω plate shown in Fig. 5(b). Small $1/2 \Omega$ unit cell high ledges are observed on the top face of the plate, whilst a much larger ledge can be seen on the lower broad face. These ledges are consistent with the two types of ledges observed by Fonda *et. al.* [16] in their studies of misfit strain accommodation surrounding Ω plates.

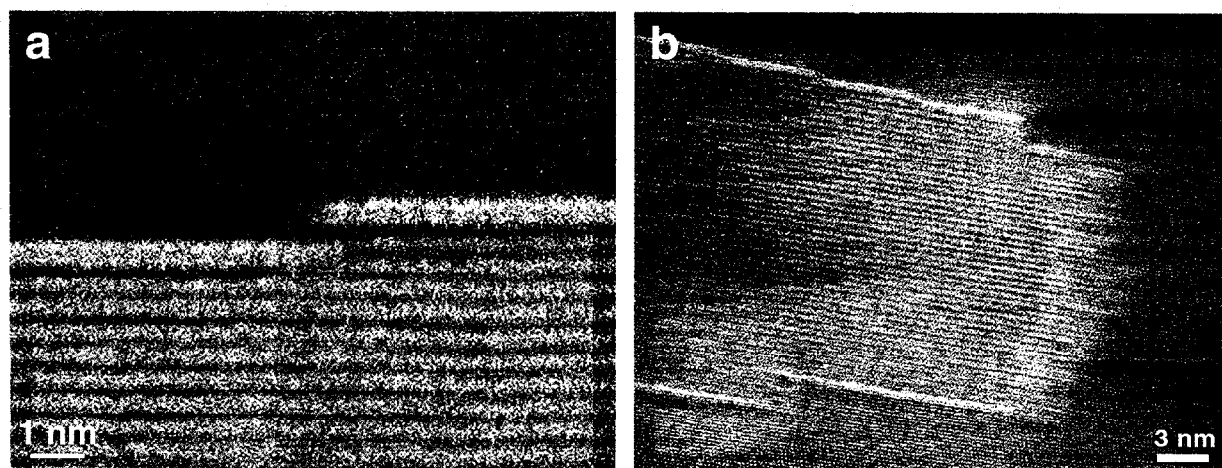


Figure 5. Z-contrast images of sample transformed (a) 72h, 250 °C and (b) 50h, 300 °C.

3.2.2 High Resolution Phase Contrast Microscopy

The Z-contrast observations indicated thickening ledges were rarely observed on Ω plates treated at 200 °C. Conventional high resolution phase contrast imaging has been used to examine the generality of this observation in samples treated for 10h and 1000h at 200 °C.

In almost all cases the plates observed did not contain any ledges. A typical example is shown in Fig. 6(a). Ten Ω plates have been documented from HRES images and the ledge density and thickness of each of the plates recorded in Table I. Of the ten plates recorded on film, only one plate contained a ledge. The ledges observed in Fig. 5(a) and on the top face in Fig. 5(b) were $1/2 \Omega$ unit cell in height and coherent with the matrix. A survey of the literature also shows that when ledges are observed on Ω plates, they are most commonly $1/2 \Omega$ unit cell in height [16]. Plate thicknesses can be determined directly from HRES images and this has been illustrated in Fig. 6(b). A high resolution simulation was performed from a model structure containing a 6.5Ω unit cell thick plate bounded by two atomic layers of mixed Ag and Mg and embedded in the Al matrix. The simulation inset is shown in Fig. 6(b). The agreement between experimental and simulated images is satisfactory and it is concluded that the plate is 6.5Ω unit cells in thickness. The thickness of each of the 10 plates examined has been evaluated and included in Table I. This information along with the number of Frank partial dislocations at the ends of the plates allows the unrelaxed misfit normal to the plate to be calculated. The plate shown in Fig. 6 is suitably oriented to directly image the Frank partial dislocations at the ends of the plate. Figs. 6(b) and (c) are enlarged images of both ends of the plate in (a). Two misfit dislocations exist at the end of this 6.5Ω unit cell thick plate and have been clearly labelled.

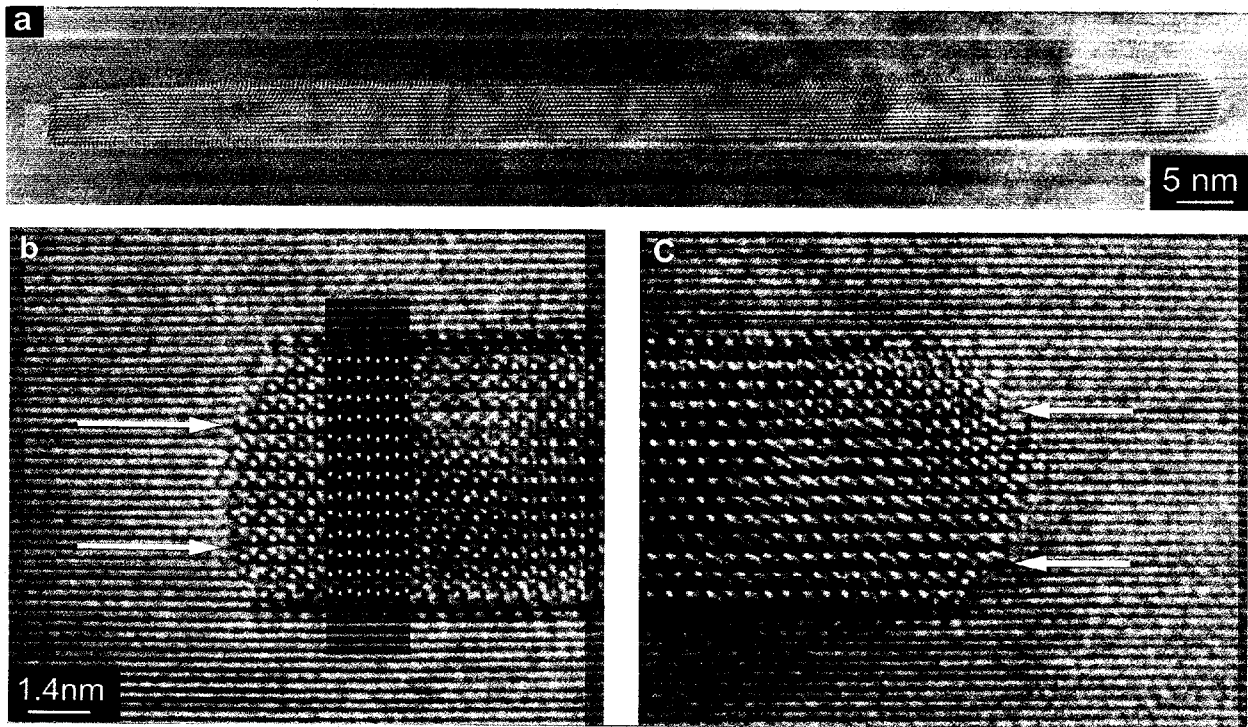


Figure 6. a) High resolution phase contrast image of an Ω plate after exposure for 1000h at 200 °C. The plate contains no ledges. $b = \langle 112 \rangle_{\alpha} // [110]_{\Omega}$ (b) High magnification image of the left end and (c) right end of the plate in (a). The ends of the plate contain two dislocations (arrowed) of type $1/3 \langle 111 \rangle_{\alpha}$, with the extra half plane in the precipitate phase.

Table I: Summary of Ω plate thickness and ledge density recorded from high resolution phase contrast images of samples treated at 200 °C.

Ω Plate	Heat Treatment Condition	Plate Thickness (Ω unit cells)	Number of coherent $1/2 \Omega$ unit cell high ledges	Inferred number of $1/3 \langle 111 \rangle_{\alpha}$ dislocations at plate ends	Unrelaxed misfit (%) in $[001]_{\Omega} \parallel [111]_{\alpha}$ direction.
1	200 °C, 10h	4	0	1	-24.6
2	200 °C, 10h	1	0	0	-18.7
3	200 °C, 10h	2.5-3.5	2 ^a	1	+3.38 -15.3
4	200 °C, 10h	2.5	0	1	+3.38
5	200 °C, 10h	3	0	1	-5.9
6	200 °C, 1000h	6	0	2	-11.9
7	200 °C, 1000h	6	0	2	-11.9
8	200 °C, 1000h	7	0	2	-30.5
9	200 °C, 1000h	6.5	0	2	-21.2
10	200 °C, 1000h	5.5	0	2	-2.6

a. The ledge on this plate is in fact a single 1Ω unit cell high coherent ledge.

4. Discussion

This study has shown that despite considerable differences in Ω plate thickening kinetics between 200 °C and 300 °C, no significant changes in the segregation behavior of Ag and Mg are observed. Two atomic layers of Ag and Mg segregation are found at the coherent broad faces of the plates. No segregation is found at the risers of thickening ledges, consistent with the observations of Reich *et al.* [17], nor is any significant segregation observed at the ends of the plates or within the plates themselves. Consequently, the necessary Ag and Mg redistribution from the broad face of the plate to the terrace of a migrating ledge (Fig. 1) must accompany ledge migration at all temperatures. Any interaction between the redistributing Ag and Mg and the flux of Cu to the ledge riser is expected to occur at all temperatures and is not considered unique to temperatures below 200 °C. Therefore, if an interaction does exist it is not considered to play the decisive role in the excellent coarsening resistance exhibited by Ω plates at temperatures up to 200 °C. The characteristic feature that distinguishes Ω plates transformed at 200 °C from those at higher temperatures is the thickening ledge density. Samples transformed at 200 °C for times greater than 10h rarely contained ledges (Table I). A large increase in thickening ledge density was observed for samples treated at 300 °C, concomitant with greatly enhanced plate thickening kinetics. The excellent coarsening resistance of Ω plates at temperatures up to 200 °C can be ascribed to a limited supply of thickening ledges.

The most commonly observed thickening ledges on Ω plates are coherent and $1/2 \Omega$ unit cell in height. Nucleation of these ledges replaces two matrix $\{111\}_\alpha$ planes and introduces a vacancy misfit of more than 0.04nm normal to the habit plane of the plate [16]. The nucleation of a coherent misfitting crystal in an elastically constrained matrix can be strongly influenced by elastic interactions with pre-existing strain fields in the matrix. Since the $1/2 \Omega$ unit cell high coherent ledge exhibits a vacancy misfit normal to the plate, the nucleation probability is highest (activation barrier is lowest) when the plates exhibit a residual interstitial misfit and increasingly less probable for increasing vacancy strains normal to the broad face of the plate. A plot of the change in unrelaxed misfit (expressed in nm) normal to the Ω plate habit plane as a function of Ω plate thickness is shown in Fig. 7. As successive coherent vacancy misfitting $1/2 \Omega$ unit cell ledges are added to the broad face of a plate, the overall vacancy misfit normal to the plate increases. This is represented by the solid line (AB) in Fig. 7. Above some critical value of this misfit¹ it becomes energetically favorable for a dislocation of the type $b=1/3[111]_\alpha$ to form with the extra half plane in the precipitate phase (e.g. Fig. 6(b)). The resulting misfit associated with the plate becomes interstitial in nature ($B \rightarrow C$, Fig. 7). Subsequent nucleation of coherent vacancy misfitting ledges reduces the interstitial misfit and the strain field normal to the broad face once again becomes vacancy in nature ($C \rightarrow D$, Fig. 7), with an associated increase in the activation barrier for coherent vacancy misfitting ledge nucleation. For those plates transformed at 200 °C and listed in Table I, the inferred number of Frank partial dislocations and the unrelaxed misfit normal to the plate have been evaluated on the basis of Fig. 7. The table shows that in all cases except plates 3 and 4, a vacancy misfit exists normal to the plate. In the case of plate 4, the misfit is interstitial, albeit only slightly. These plates contain no ledges because the nucleation barrier for a coherent vacancy misfitting ledge in a pre-existing vacancy field is prohibitively large. Plate 3 provides an interesting example. It was the only plate observed with a ledge, and the ledge is a single coherent full Ω unit cell in height. The plate was initially 2.5 cells thick, corresponding to an interstitial strain field (E , Fig. 7), but after propagation of the ledge, the plate is 3.5 cells thick with a strong vacancy misfit (F , Fig. 7). Nucleation of the coherent

1. The critical misfit normal to the plate corresponding with the formation of a Frank partial dislocation of the type $b=1/3[111]_\alpha$ may depend on plate thickness. At very small plate thicknesses, the plate is expected to behave as an elastically constrained thin film, but as the plate thickens the elastic properties of the plate would be expected to more closely approach those of bulk Ω .

vacancy misfitting ledge is assisted through mitigation of the interstitial strain field normal to the plate. In all cases observed, plates that contain ledges have a residual interstitial misfit (or only slightly vacancy) and those that contain no ledges exhibit a vacancy misfit¹. Most of the plates listed in Table I exhibit strong vacancy misfits, conditions very unfavorable for the nucleation of coherent vacancy misfitting ledges. It is concluded that nucleation of coherent ledges during the coarsening stages of Ω plate thickening are dominated by strain energy considerations and that this effect is responsible for the excellent coarsening resistance of Ω plates at temperatures up to 200 °C.

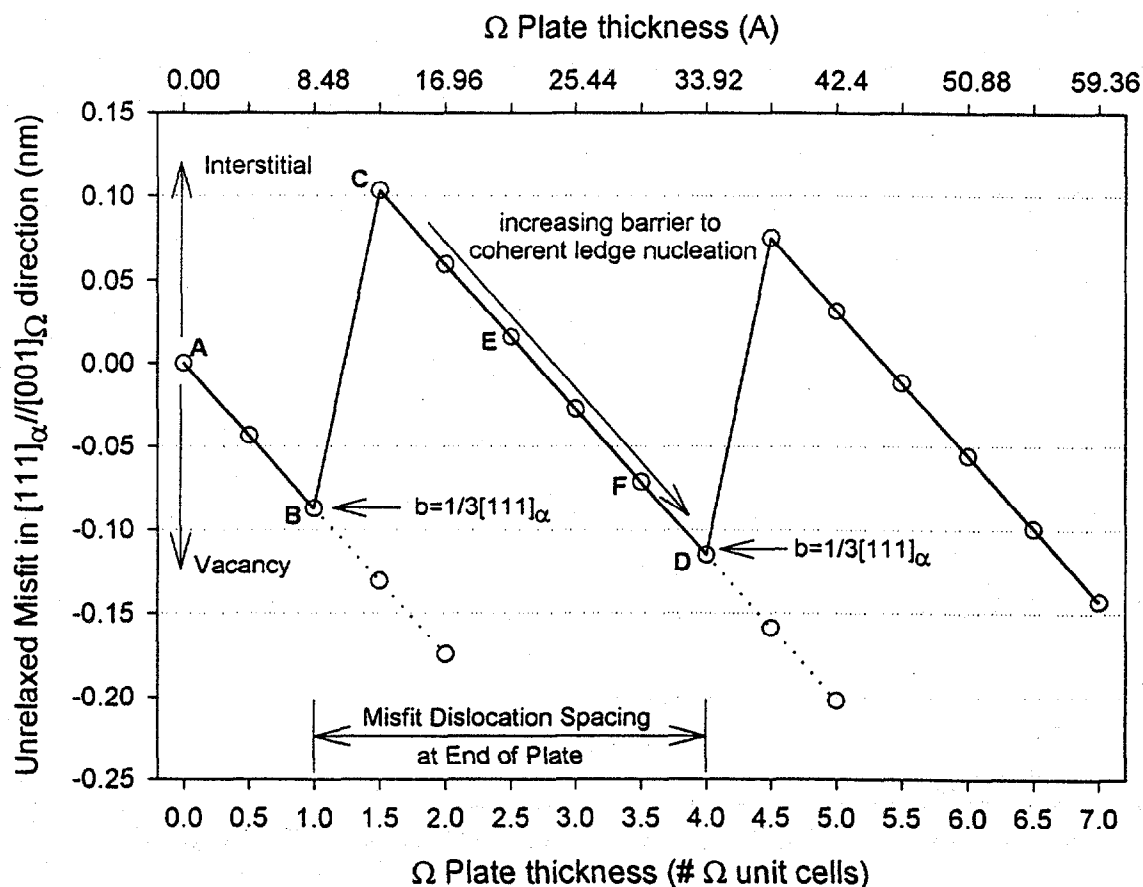


Figure 7. Plot of the change in unrelaxed misfit (nm) normal to the Ω plate habit plane as a function of Ω plate thickness.

The analysis presented above applies only at relatively small plate thicknesses. The matrix dislocation density greatly increased during the later stages of thickening of Ω plates at 250 °C and 300 °C and these dislocations interacted strongly with both the edges and the broad faces of the plates, presumably to aid in the accommodation of strain associated with the plate. The regime of thickening that includes the generation of matrix dislocations and their interaction with the strain fields of the plates is beyond the scope of this study.

1. Fonda *et al* [16] observed that the average spacing of Frank partial dislocations at the ends of thick plates was 2.5-3.0 Ω unit cells. This is an *average* spacing and was used to construct Fig. 7. Deviations from this average spacing may reveal plate thicknesses that appear inconsistent with the arguments presented above on the basis of Fig. 7. In those cases, direct observation of the number of dislocations at the ends of the plates is necessary.

5. Conclusions

Z-contrast observations revealed two atomic layers of Ag and Mg segregation to the $(001)_{\Omega} \parallel (111)_{\alpha}$ interphase boundary at all times and temperatures examined. No segregation was found to the risers of thickening ledges or to the ends of the plates. No Ag or Mg was detected in any significant quantities within the plate at any time. The necessary Ag and Mg redistribution from the broad face of the plate to the terrace of the migrating thickening ledge must accompany ledge migration at all temperatures and is not considered to play a decisive role in accounting for the excellent coarsening resistance of Ω plates at temperatures up to 200 °C. Consistent with previous investigations of the thickening kinetics of precipitate plates in Al-alloys [13, 14, 15], the thickening of Ω plates is restricted by a limited supply of ledges. The density of thickening ledges on plates transformed for times longer than 10h at 200 °C was very low, usually zero. A large increase in ledge density is associated with the increase in thickening kinetics at 250 °C and 300 °C. The prohibitively high barrier to coherent ledge nucleation on the broad faces of plates aged at 200 °C arises from the contribution to the total free energy change attending nucleation from elastic interactions between the misfitting coherent ledges and the significant strain field that can exist normal to the broad face of the Ω plate.

6. References

1. Auld, J. H. and Vietz, J. T., in *The Mechanism of Phase Transformations in Crystalline solids, Monograph and Report Series*, No. 33, pp. 77-79. Inst. Metals, London (1969).
2. Taylor, J. A., Parker, B. A and Polmear, I. J., *Metals Sci.*, 1978, **12**, 478.
3. Chester, R. J. and Polmear, I. J., *Micron*, 1980, **11**, 311.
4. Chester, R. J. and Polmear, I. J., in *The Metallurgy of Light Alloys*, pp. 75-81, Inst. Metals, London (1983).
5. Auld, J. H., *Mater. Sci. Technol.*, 1986, **2**, 784.
6. Scott, V. D., Kerry, S. and Trumper, R. L., *Mater. Sci. Technol.*, 1987, **3**, 827.
7. Garg, A. and Howe, J. M., *Acta metall.*, 1991, **39**, 1939.
8. Knowles, K. M. and Stobbs, W. M., *Acta crystallogr.*, 1988, **B44**, 207.
9. Muddle, B. C. and Polmear, I. J., *Acta metall.*, 1989, **37**, 777.
10. Polmear, I. J. and Couper, M. J., *Metall. Trans.*, 1988, **19A**, 1027.
11. Ringer, S. P., Yeung, W., Muddle, B. C. Polmear, I. J., *Acta metall. mater.*, 1994, **42**, 1715.
12. Aaronson, H. I., in *Decomposition of Austenite by Diffusional Processes*, pp. 387-548, Eds. Zackay, V. F. and Aaronson, H. I., Interscience, (1962).
13. Aaronson, H. I. and Laird, C., *Trans. AIME*, 1968, **242**, 1437.
14. Sankaran, R. and Laird, C., *Acta Metallurgica*, 1974, **22**, 957.
15. Laird, C. and Aaronson, H. I., *Acta Metallurgica*, 1969, **17**, 505.
16. Fonda, R. W, Cassada, W. A and Shiflet, G. J., *Acta metall. mater.*, 1992, **40**, 2539.
17. Reich, L., Murayama, M. and Hono, K., *Acta mater.*, 1998, **46**, 6053.
18. Software development by Roar Kilaas, National Center for Electron Microscopy (NCEM), Lawrence Berkeley National Laboratory, Berkeley, CA.
19. Pennycook, S. J. and Jesson, D. E., *Phys. Rev. Lett.*, 1990, **64**, 938-941.
20. Pennycook, S. J. and Nellist, P. D., in *Impact of Electron and Scanning Probe Microscopy on Materials Research*, pp. 161-207, Ed.'s Rickerby, D. G., Valdré, U. and Valdré, G., Kluwer Academic Publishers, The Netherlands, 1999.